Dynamic regulation of the tryptophan operon: A modeling study and comparison with experimental data

Moisés Santillán *

Michael C. Mackey †

Department of Physiology and Centre for Nonlinear Dynamics, McGill University
McIntyre Medical Sciences Building
3655 Drummond Street, H3G 1Y6 Montreal QC, CANADA

Abstract

A mathematical model for regulation of the tryptophan operon is presented. This model takes into account repression, feedback enzyme inhibition, and transcriptional attenuation. Special attention is given to model parameter estimation based on experimental data. The model's system of delay differential equations is numerically solved, and the results are compared with experimental data on the temporal evolution of enzyme activity in cultures of *E. coli* after a nutritional shift (minimal + tryptophan medium to minimal medium). Good agreement is obtained between the numeric simulations and the experimental results for wild type *E. coli*, as well as for two different mutant strains.

1 Introduction

The term operon was first proposed in a short paper in the proceedings of the French Academy of Sciences in 1960 [1]. From this paper, the so-called general theory of the operon was developed. This theory suggested that all genes are controlled by means of operons where an operon consists of a set of genes preceded by a small DNA segment (the operator), in which the regulatory process takes place. According to the original theory of the operon, there was one single feedback regulatory mechanism, known as repression: a repressor molecule binds the operator, inhibiting transcription initiation. Later, it was discovered that the regulation of genes is a much more complicated process. Indeed it is not possible to talk of a general regulatory mechanism, as there are many, and they vary from operon to operon. The current definition of operon is a single transcriptional unit, no matter what its regulatory system is. The regulatory system need not be included [2]. Despite modifications, the development of the operon concept is considered one of the landmark events in the history of molecular biology.

Shortly after the operon concept was presented, a mathematical model for it was proposed [3]. Bliss *et al.* [4] proposed a more detailed model for the tryptophan operon that considered repression and feedback inhibition. The system's inherent time delays due to transcription and translation were also taken into account. More recent experimental results reveal that the dynamics of the interaction between repressor and tryptophan molecules are different than considered in Bliss' model. Furthermore, the Bliss model did not take into account another regulatory mechanism at the DNA level, which was discovered later and is called transcriptional attenuation. More recently, other models have been proposed [5, 6, 7]. They take into account (with more detail) the interactions among the repressor molecules, the operon, and the operon end-product (tryptophan). Nevertheless, they consider neither feedback inhibition nor transcriptional attenuation, and neglect the inherent time delays.

We present a mathematical model of the tryptophan operon regulatory system. This model considers repression, enzyme feedback inhibition, and transcriptional attenuation, as well as the system's inherent time delays. In Section 2, an outline of the mathematical model is presented. A list of the model variables and symbols is given in Table 1. The model equations are shown in Table 2. A list of all the parameters and their estimated values is given in Table 3. The variables' steady-state values are presented in Table 4. In Section 3, the numerical method used to solve the model equations is described. The pro-

*Permanent address: *Esc. Sup. de Física y Matemáticas, Instituto Politécnico Nacional, 07738, México D.F. MÉXICO*

†Corresponding author [tel: (514) 398-4336; fax: (514) 398-7452; e-mail mackey@cnd.mcgill.ca; 3655 Drummond Street, Room 1124, Montreal, Quebec, CANADA H3G 1Y6]

cedure to numerically simulate a given set of experiments and the comparison of the theory with the experiment are given. Some concluding remarks are given in Section 4, along with a discussion about the feasibility of the model and possible future directions.

Supplementary material is given in two appendices. The equation for the dynamics of repression is derived in Appendix A. This is a partial result in the development of the model. The estimation of all the model parameters is described in Appendix B.

2 The model

In this section we introduce a mathematical model of the *trp* operon regulatory system. A schematic representation of this regulatory system is given in Figure 1. As any other model, the present one is oversimplified in some sense. Many simplifying assumptions (discussed below) are made during its development. However, it is our premise that the model still considers enough of the system essential characteristics, in order to reproduce some experimental dynamic observations. In Table 1, a list of the model independent variables is presented. The exact meaning of each one is discussed in the forthcoming paragraphs.

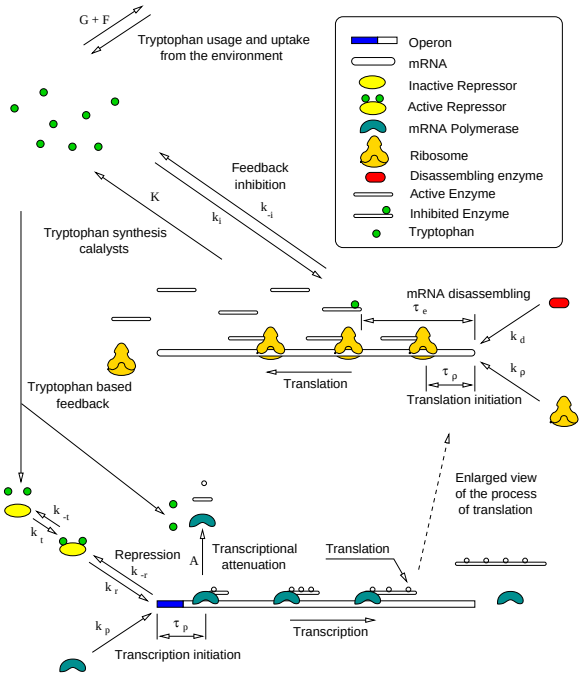

Figure 1: Schematic representation of the tryptophan operon regulatory system. See the text for details.

For the purpose of the present model, the tryptophan operon is considered to be constituted by the major structural genes, preceded by a controlling section, where both repression and transcription initiation take place. Consider all the *trp* operons in a bacterial (*E. coli*) culture. The controlling sections can be in one of three different states: Free (O_F), repressed (O_R), or bound by a *mRNA* polymerase (O_P) (here, the same symbols are employed to represent the chemical species and their concentration, unless otherwise stated). We assume that there is a single type of repressor molecule, produced by the *trpR* operon, whose active form competes with *mRNA* polymerase (*mRNAP*) to bind free controlling sections. Let R_A denote the concentration of active repressor molecules. The repression process is assumed in this model to be a first order reversible chemical reaction with forward and backward rate constants k_r and k_{-r}, respectively. These constants are estimated in Appendix B and tabulated in Table 3. On the other hand, when a *mRNAP* binds a free operon, the *DNA-mRNAP* complex has to undergo a series of isomerizations before it can assemble the first *mRNA* nucleotide. We assume that this whole process takes place with a rate proportional to the free operon and *mRNA* polymerase (P) concentrations, with a rate constant represented by k_p. After that, the *mRNAP* starts moving along the operon, synthesizing the *mRNA* chain. A time τ_p after the *mRNAP* binds the controlling section, it has moved far enough to free the operon, which is then available to be bound by another *mRNAP* or a repressor molecule. The parameters k_p, P, and τ_p are estimated in Appendix B and tabulated in Table 3. All these considerations, along with the assumption that the bacterial culture is exponentially growing at a rate μ, allow us to write down the equations governing the dynamics of O_F. In doing this, we point out that the estimated values of k_r, k_{-r}, and k_p reveal that the binding rate of repressor molecules to free operons is two orders of magnitude larger than the corresponding binding rate of *mRNAP*'s. This fact justifies a quasi-steady

O	Total operon concentration
O_F	Free operon concentration
M_F	Free *mRNA* concentration
E	Total enzyme concentration
E_A	Active enzyme concentration
T	Tryptophan concentration
R	Total repressor concentration
R_A	Active repressor concentration
P	*mRNA* polymerase concentration
ρ	ribosomal concentration
D	*mRNA* destroying enzyme concentration

Table 1: Model variables and symbols

state assumption for the repression process. From all this, the resulting equation for the dynamics of O_F is given by Equation (1) of Table 2. The details of its derivation are given in Appendix A.

$$\frac{dO_F}{dt} = \frac{K_r}{K_r + R_A(T)}\Big\{\mu O - k_p P\big[O_F(t) - O_F(t-\tau_p)e^{-\mu\tau_p}\big]\Big\} - \mu O_F(t) \quad (1)$$

$$A(T) = b\left(1 - e^{-T(t)/c}\right) \quad (2)$$

$$\frac{dM_F}{dt} = k_p P O_F(t-\tau_m)e^{-\mu\tau_m}\big[1 - A(T)\big] - k_\rho \rho\big[M_F(t) - M_F(t-\tau_\rho)e^{-\mu\tau_\rho}\big] - \big(k_d D + \mu\big)M_F(t) \quad (3)$$

$$\frac{dE}{dt} = \frac{1}{2}k_\rho \rho M_F(t-\tau_e)e^{-\mu\tau_e} - \big(\gamma + \mu\big)E(t) \quad (4)$$

$$E_A(E,T) = \frac{K_i^{n_H}}{K_i^{n_H} + T^{n_H}(t)}E(t) \quad (5)$$

$$R_A(T) = \frac{T(t)}{T(t) + K_t}R \quad (6)$$

$$G(T) = g\frac{T(t)}{T(t) + K_g} \quad (7)$$

$$F(T, T_{\text{ext}}) = d\frac{T_{\text{ext}}}{e + T_{\text{ext}}\left[1 + T(t)/f\right]} \quad (8)$$

$$\frac{dT}{dt} = K E_A(E,T) - G(T) + F(T, T_{\text{ext}}) - \mu T(t) \quad (9)$$

Table 2: Equations describing the evolution of the variables O_F, M_F, E, and T. See the text for the details on their derivation

The *mRNA* molecules synthesized by transcription encode five different polypeptides. These polypeptides are used to build up the enzymes which participate in the catalytic pathway that synthesizes tryptophan from chorismic acid. The first enzyme in this pathway (anthranilate synthase) is a complex of two *TrpE* and two *TrpD* polypeptides, which are respectively the first and second proteins encoded by the *trp mRNA*. From the regulatory point of view, anthranilate synthase is the most important of the enzymes in the catalytic pathway. This is because it catalyzes the first reaction in the tryptophan synthesis pathway and because it is subject to feedback inhibition by tryptophan. Since there is evidence supporting the assumption that the production rates of all of the five polypeptides encoded by the *trp mRNA* are very similar under normal conditions [8], we focus on the production of *TrpE* polypeptide and assume that the anthranilate synthase production rate is just one half that of *TrpE*. Let M_F represent the concentration of free *TrpE*-related ribosome binding sites. M_F increases due to transcription. Nevertheless, not all of the *mRNAP*'s that initiate transcription produce functional *mRNA*'s. Many of them terminate transcription prematurely depending on the availability of charged $tRNA^{Trp}$. The higher the concentration of charged $tRNA^{trp}$, the more probable that a transcribing *mRNAP* aborts transcription at a premature stage. This regulatory mechanism is known as transcriptional attenuation. Since the amount of charged $tRNA^{Trp}$ depends on the tryptophan concentration, we assume that the probability of premature transcription termination $\big(A(T)\big)$ is just a function of the tryptophan concentration. The functional form of $A(T)$ is given by Equation (2) of Table 2 and discussed in Appendix B. From this, if τ_m is the time it takes for a *mRNAP* to assemble a functional *TrpE*-related ribosome binding site, the M_F production rate equals the rate of *mRNAP*'s that bound free operons a time τ_m ago $\big(k_p P O_F(t-\tau_m)\big)$ times a factor $e^{-\mu\tau_m}$, standing for the dilution due to the exponential growth, times the probability of a just bound *mRNAP* to produce a functional *mRNA* $\big(1 - A(T)\big)$. After a ribosome binds a free *TrpE*-related binding site, the *mRNA*-ribosome complex must suffer a series of isomerizations before it can assemble the first peptide bound. Here we assume that this whole process takes place with a rate proportional to M_F and to the ribosomal concentration ρ, with a rate constant denoted by k_ρ. After that, the ribosome moves along the *mRNA* performing translation. A time τ_ρ after binding, the ribosome has moved far enough to free the binding site. Thus, M_F is affected by translation initiation in the following way: In an infinitesimal period of time it decreases in an amount equal to the rate of ribosome binding and initiating translation, and increases by an amount equal to the rate that ribosomes bound and initiated translation a time τ_ρ ago, times the corresponding dilution factor. *mRNA* degradation is an active process carried out by different types of enzymes [9]. Following McAdams and Arkin [10] we consider in this model a single pool of *mRNA* destroying enzymes (D) and assume that they cause M_F to decrease with a rate proportional to M_F and D, being the rate constant denoted by k_d. The equation governing the dynamics of M_F derived from all the above considerations and the exponential growth assumption is given by Equation (3) of Table 2.

Let E denote the anthranilate synthase concentra-

R	$\simeq$	$0.8\,\mu$M	O	$\simeq$	$3.32\times10^{-3}\,\mu$M
P	$\simeq$	$2.6\,\mu$M	k_{-r}	$\simeq$	$1.2\,\text{min}^{-1}$
ρ	$\simeq$	$2.9\,\mu$M	k_r	$\simeq$	$460\,\mu\text{M}^{-1}\text{min}^{-1}$
τ_p	$\simeq$	$0.1\,$min	k_{-i}	$\simeq$	$720\,\text{min}^{-1}$
τ_m	$\simeq$	$0.1\,$min	k_i	$\simeq$	$176\,\mu\text{M}^{-1}\text{min}^{-1}$
τ_ρ	$\simeq$	$0.05\,$min	k_{-t}	$\simeq$	$2.1\times10^{4}\text{min}^{-1}$
τ_e	$\simeq$	$0.66\,$min	k_t	$\simeq$	$348\,\mu\text{M}^{-1}\text{min}^{-1}$
γ	$\simeq$	$0\,\text{min}^{-1}$	k_p	$\simeq$	$3.9\,\mu\text{M}^{-1}\text{min}^{-1}$
k_dD	$\simeq$	$0.6\,\text{min}^{-1}$	k_ρ	$\simeq$	$6.9\,\mu\text{M}^{-1}\text{min}^{-1}$
n_H	$\simeq$	1.2	μ	$\simeq$	$1.0\times10^{-2}\,\text{min}^{-1}$
b	$\simeq$	0.85	c	$\simeq$	$4.0\times10^{-2}\,\mu$M
K_g	$\simeq$	$0.2\,\mu$M	g	$\simeq$	$25\,\mu\text{M}\,\text{min}^{-1}$
e	$\simeq$	$0.9\,\mu$M	d	$\simeq$	$23.5\,\mu\text{M}\,\text{min}^{-1}$
f	$\simeq$	$380\,\mu$M	K	$\simeq$	$126.4\,\text{min}^{-1}$

Table 3: The model parameters as estimated in Appendix B

tion. As mentioned above, this enzyme is the most important from a regulatory point of view because is the first one to catalyze a reaction in the *Trp* synthesis catalytic pathway and because it is subject to feedback inhibition by tryptophan. Anthranilate synthase is a complex of two *TrpE* and two *TrpD* polypeptides. However, we focus on the *TrpE* production only (based on the fact that the production rate of all the *trp* polypeptides is similar under normal conditions [8]) and assume that the anthranilate synthase production rate is just one half that of *TrpE*. If τ_e is the time it takes for a ribosome to synthesize a *TrpE* polypeptide, the *TrpE* production rate equals the ribosome binding rate delayed a time τ_e, times the corresponding dilution factor. From this, the exponential growth assumption and supposing that enzymes are degraded at a rate given by γE (γ is the enzymatic degradation rate constant), it is possible to derive the equation governing the dynamics of E, given by Equation (4) of Table 2.

Anthranilate synthase is feedback inhibited by tryptophan. This is achieved by the binding of two *Trp* molecules to each one of the *TrpE* subunits of anthranilate synthase. The binding of these two *Trp* molecules is not instantaneous but sequential and cooperative, with a Hill coefficient of $n_H \simeq 1.2$ [11]. The forward (k_i) and backward (k_{-i}) reaction rate constants of the *Trp* feedback inhibition of anthranilate synthase reaction are estimated in Appendix B and tabulated in Table 3. A comparison of k_i and k_{-i} with $k_\rho\rho$, μ, and γ (also tabulated in Table 3) reveals that the feedback inhibition of anthranilate synthase is at least two orders of magnitude larger than the enzymatic production, degradation and dilution processes. This in turn justifies a quasi-steady state assumption for the feedback inhibition process. From this, the concentration of active (non-inhibited) anthranilate synthase can be calculated as given by Equation (5) of Table 2 [4], where $K_i = k_{-i}/k_i$.

The tryptophan operon repressor *TrpR* is produced by an independent operon which is negatively feedback regulated by active *TrpR*. When produced, *TrpR* molecules are inactive (aporepressor) and unable to repress the *trp* and *trpR* operons. It becomes active when is bound by two tryptophan molecules at two independent sites with identical affinities and no cooperativity [12, 13, 14, 15]. The value of the forward (k_t) and backward (k_{-t}) rate constants of the repressor activation reaction are estimated in Appendix B and given in Table 3. From this, we observe that the repressor activation rate is about two orders of magnitude larger than the rate of active repressor molecules binding free operons and initiating transcription. Repression activation can then be assumed to take place in a quasi-steady state. All these determine the relation between the active repressor concentration, the tryptophan concentration, and the total repressor concentration (R) given by Equation (6) of Table 2, where $K_t = k_{-t}/k_t$. The synthesis of the *trp* aporepressor increases when tryptophan is growth limiting, because the repressor autoregulates its own synthesis. However, we assume that the total repressor concentration is constant. We do this for the sake of simplicity and because of the lack of enough experimental data in that respect.

Tryptophan is synthesized from chorismic acid by a series of reactions catalyzed by enzymes built up with the *trp* polypeptides. As argued above, of all the enzymes, the most important from a regulatory point of view is anthranilate synthase. From this, we assume that *Trp* production is mostly dependent on the active anthranilate synthase concentration (E_A). Indeed, the *Trp* production rate is taken as KE_A, with K a constant to be estimated. Tryptophan is involved in the activation of the *trp* repressor and in the feedback inhibition of anthranilate synthase. However, here we assume both reactions take place under quasi-steady state conditions. This means that the rate of tryptophan usage by the forward reactions equals the rate of tryptophan dissociation by the backward reactions, and therefore that the *Trp* concentration is not affected by the repressor activation and feedback inhibition of anthranilate synthase processes.

Tryptophan is employed in the production of the proteins the bacteria need to grow. The rate of tryptophan usage in protein production is modeled by the function $G(T)$ given by Equation (7) of Table

$\overline{O_F}$	$\simeq$	$1.54 \times 10^{-4}\,\mu$M
$\overline{M_F}$	$\simeq$	$3.78 \times 10^{-4}\,\mu$M
$\overline{E}$	$\simeq$	$0.378\,\mu$M
$\overline{T}$	$\simeq$	$4.1\,\mu$M

Table 4: The steady-state values of the model variables corresponding to the parameter values shown in Table 3 and a medium without tryptophan

2. The functional form of $G(T)$ is discussed in Appendix B. *E. coli* are capable of synthesizing three different permeases responsible for the active uptake of tryptophan from the environment [16]. The function $F(T, T_{\text{ext}})$ that stands for the rate of tryptophan uptake (T_{ext} represents the external tryptophan concentration) is studied in Appendix B and given by Equation (8) of Table 2. The equation for the dynamics of T derived from all these considerations is given by Equation (9) of Table 2.

Equations (1)-(9) constitute the complete system of time-delay differential equations that model the *trp* operon regulatory system. They have 28 parameters which must be estimated for the model to be completely specified. We emphasize the importance of having proper estimations for all of these parameters. Otherwise, it is impossible to expect the model to reproduce the behavior of the real system. The complete procedure followed to estimate the model's parameters is described in Appendix B. These parameters are tabulated in Table 3. The steady-state values of the model variables are shown in Table 4, and these steady-state values correspond to bacteria growing in a medium without external tryptophan.

3 Numerical results and comparison with experiments

Having the estimated parameters of Table 3, the system of differential delay equations was solved numerically using a fourth order Runge-Kutta method. The program was implemented in Fortran. The convergence of the program was tested empirically. A time step of 0.01 min was found to represent a good compromise between accuracy and speed.

Yanofsky and Horn [17] report experiments with wild and mutant strains of *E. coli* CY15000 strain. These experiments consisted of growing bacteria in the minimal medium of Vogel and Bonner [18] plus tryptophan during a time long enough for the culture to reach the steady state. Then the bacteria were washed and put into minimal media only. The response of the anthranilate synthase enzyme activity was measured as a function of time.

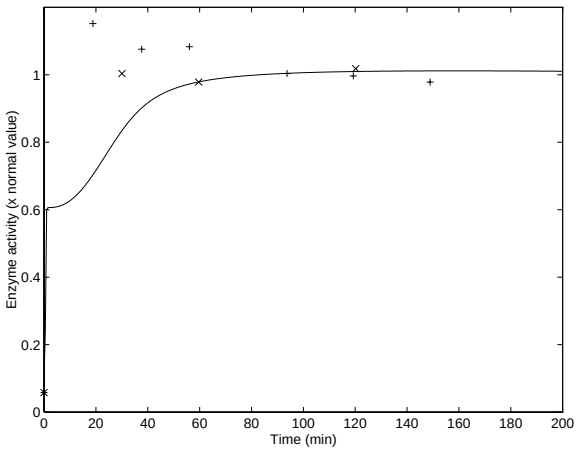

Figure 2: Enzyme activity *vs.* time after a nutritional shift (minimal + tryptophan medium to minimal medium), with wild strain cultures of *E. coli*. Two different sets of experimental results (crosses and pluses) as well as the model simulation (solid line), with the parameters of Table 3, are presented. The simulation was calculated by numerically solving the differential equations. The selection of initial conditions is described in the text. The normal enzyme activity is that of the steady state in a medium without tryptophan.

To simulate these experiments, we begin by setting all the variables at their normal steady state values (Table 4). These steady state values correspond to the parameters in Table 3 and a medium with no external tryptophan. For the wild strain of *E. coli*, all the parameters have their normal values (Table 3). The internal tryptophan concentration ($\overline{T}$) estimated in Appendix B for a medium without tryptophan is about $4.1\,\mu$M. The minimal plus *Trp* media Yanofsky and Horn [17] employed in their experiments had a tryptophan concentration of $100\,\mu$g per milliliter of minimal media, which corresponds to about four hundred times the value of $\overline{T}$. Based on this, we set the external *trp* concentration $T_{ext} = 400 \times \overline{T}$ to simulate the growth of the bacteria culture in the minimal plus tryptophan medium. Then the system of differential delay equations is numerically solved until the solution reaches a steady state. To simulate the shift of the bacteria to the minimal medium, we ran another numerical experiment where the initial conditions are the steady state values of the variables in the minimal plus tryptophan medium solution and the external *Trp* concentration is null. During this second numerical experiment, the enzyme activity [the number of tryptophan molecules produced per unit time, $KE_A(t)$] is plotted as a function of time.

The results of two different experiments from [17] with a normal strain of *E. coli* are plotted (with crosses and pluses) in Figure 2. The results of the

numerical simulation are plotted with a solid line in the same figure. Since Yanofsky and Horn [17] report values of enzyme activity in arbitrary units, to compare with our simulation the experimental values were scaled so the steady state values of the experiment and the model were equal.

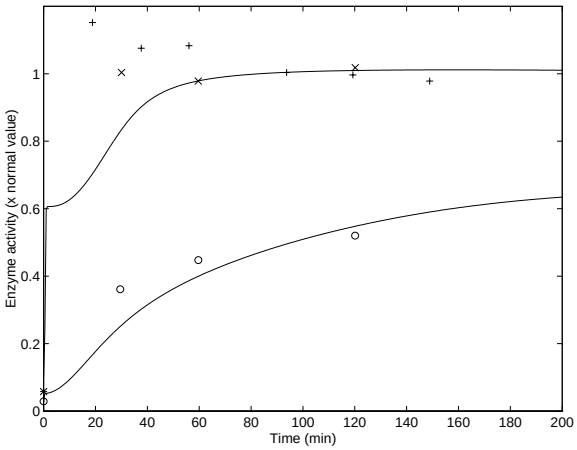

Figure 3: Enzyme activity *vs.* time after a nutritional shift (minimal + tryptophan medium to minimal medium), with wild strain (crosses and pluses) and *trpL29* mutated (circles) cultures of *E. coli*. The numerical simulations for each strain (solid lines), are also shown. The simulation for the *trpL29* mutated strain was calculated by numerically solving the differential equations with the parameters estimated in Table 3, except for the parameter k_p which was decreased to 0.04 times the normal value to simulate the mutation. The selection of initial conditions is described in the text. The normal enzyme activity is that of the wild-strain steady state in a medium with no tryptophan.

Yanofsky and Horn also report similar experiments with *trpL29* and *trpL75* mutant strains of *E. coli*. The *trpL29* mutant strain has a mutation A to G at bp 29 in the leader region of the *trp* operon. This change replaces the leader peptide start codon by GUG, and decreases operon expression in cells growing in the presence or absence of tryptophan. This mutation can be interpreted as decreasing the rate constant k_p, which determines the rate of polymerase binding free operons and initiating transcription. We found by trial and error that with a k_p equal to 0.04 times the normal value the numerical results fit the experimental data. To compare the experimental results and the model predictions, the experimental results were again scaled by the same factor as those of the normal strain. The results are shown in Figure 3. The experimental results of this *trpL29* strain are plotted with circles. The wild strain data and simulation are also shown for comparison.

The strain *trpL75* of *E. coli* has a mutation of G to A at bp 75 in the leader region of the *trp* operon. This change decreases the stability of the

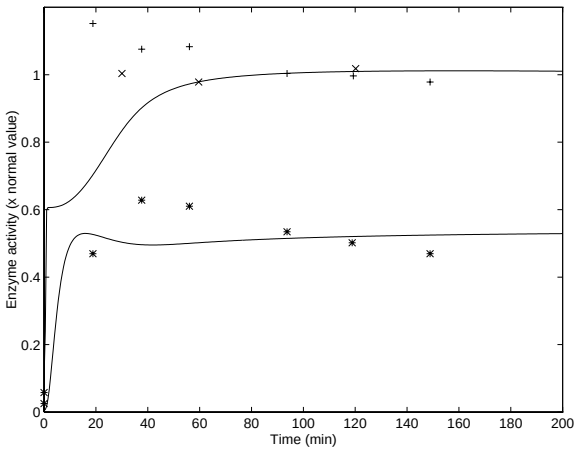

Figure 4: Enzyme activity *vs.* time after a nutritional shift (minimal + tryptophan medium to minimal medium), with wild strain (crosses and pluses) and *trpL75* mutated (asterisks) cultures of *E. coli*. The numerical simulations for each strain (solid line), are also shown. The simulation for the *trpL75* mutated strain was calculated by numerically solving the differential equations, with the parameters of Table 3, except parameter b, which was increased to 0.9996 to simulate the mutation. The selection of initial conditions is described in the text. The normal enzyme activity is that of the wild-strain steady state, in a medium with no tryptophan.

transcription antiterminator structure, and increases transcription termination at the attenuator. Consequently, it decreases operon expression of cells growing in the presence or absence of tryptophan. The probability that transcription is terminated at the attenuator is given in the model by the function $A(T) = b\big[1 - \exp\left(-T/c\right)\big]$. Therefore, an increase in the parameter b implies that the probability of transcription termination increases for every tryptophan concentration. The mutation of the *trpL75* strain was then simulated by increasing the value of b by trial and error up to 0.9996. With this value, the simulation fits the experimental data reasonably well. The experimental results (asterisks) and the simulation results for this strain are shown in Figure 4, along with those corresponding to the normal strain. In this case, the experimental results are also scaled by the same factor as those of the normal strain.

4 Concluding remarks

We have developed a mathematical model of the *trp* operon regulatory system. In this model, the following regulatory mechanisms are considered: Repression, feedback inhibition of anthranilate synthase by tryptophan, and transcriptional attenuation. However, some other features are ignored or simplified. The most important to our consideration are: Only

one of the enzymes participating in the tryptophan synthesis catalytic pathway is considered (anthranilate synthase). A single type of repressor molecules (the end-product of the *trpR* operon) is taken into account. The total (active + inactive) repressor concentration is assumed constant, despite the fact that the *trpR* operon is negatively feedback regulated by active *TrpR* and thus, the synthesis of the *trp* aporepressor increases when tryptophan is growth limiting. The production rate of anthranilate synthase is assumed to be one half that of *TrpE*. These simplifying assumptions are particularly delicate under conditions of low tryptophan concentration because the synthesis of aporepressor molecules is increased and because the production of the *trp* polypeptides is affected since some of them have *Trp* residues. Although there are more simplifying assumptions (explained in Section 2), we consider that they do not affect the model behavior as the above ones do. Special attention was given to the estimation of the model parameters.

Comparison of the model simulations with experimental results reveals that despite the simplifying assumptions, the model qualitatively reproduces the enzyme activity dynamic response of wild and, *trpL29* and *trpL75* mutant cultures of *E. coli* when they are shift from a minimal plus tryptophan to a minimal medium. As seen in Figures 2, 3, and 4, the steady-state values are recovered for all the strains. The relaxation times are also qualitatively reproduced by the model. Nevertheless, the relaxation time predicted by the model is larger than the real one in the case of the wild strain. Better agreement is observed for the *trpL29* mutant strain. In the *trpL75* mutant strain experimental results, a bump is observed before the steady state is reached. The model also predicts a bump, but it is smaller and shorter in duration. All these differences between the experiments and the model results may be due to the simplifying assumptions or to a deficient estimation of some parameters.

In conclusion, although the comparisons reported here are not sufficient to assert that the present model is accurate in all detail, the results are sufficiently encouraging to prompt us to seek further sources of data for comparison. Future work would mean an interactive cooperation between experiment and theory to obtain better parameter estimations, to test the dynamic response of the model under different circumstances, and to improve the model formulation.

5 Acknowledgments

We would like to thank Prof. Charles Yanofsky for suggesting the experimental data against which we could test our model predictions. This work was supported by CONACyT and COFAA-IPN (México), the Natural Sciences and Engineering Research Council (NSERC grant OGP-0036920, Canada), the Alexander von Humboldt Stiftung, and Le Fonds pour la Formation de Chercheurs et l'Aide à la Recherche (FCAR grant 98ER1057, Québec).

References

[1] Jacob. F; Perrin, D.; Sanchez, C.; and Monod, J. (1960). L'Operon: groupe de gène à expression par un operatour. C. R. Seances Acad. Sci. **250:** 1727-1729.

[2] Beckwith, J. (1996) The operon: an historical account. In: *Escherichia coli* and *Salmonella thyphymurium*: Cellular and molecular biology (Neidhart, F. C. et al. editors) Vol. 2, pp 1553-1569. Washington D. C., American Society for Microbiology.

[3] Goodwin (1965) Oscillatory behaviour in enzymatic control process. Adv. Enz. Regul. **3:** 425-438.

[4] Bliss, R. D.; Painter R. P.; & Marr, A. G. (1982). Role of feedback inhibition in stabilizing the classical operon. J. Theor. Biol. **97,** 177-193.

[5] Sinha, S. (1988) Theoretical study of tryptophan operon: Application in microbial technology. Biotechnol. Bioeng. **31:** 117-124.

[6] Sen, A. K. and Liu W. (1989) Dynamic analysis of genetic control and regulation of amino acid synthesis: the tryptophan operon in *Escherichia coli*. Biotechnol. Bioeng. **35:** 185-194.

[7] Xiu, Z. L.; Zeng A. P.; & Deckwer, W. D. (1997) Model analysis concerning the effects of growth rate and intracellular tryptophan level on the stability and dynamics of tryptophan biosynthesis in bacteria. J. Biotechnol. **58:** 125-140.

[8] Yanofsky, C. & Crawford, I. P. (1987). The tryptophan operon. In: *Escherichia coli* and *Salmonella thyphymurium*: Cellular and molecular biology (Neidhart, F. C. *et al.* editors) Vol. 2, pp 1454-1472. Washington D. C., American Society for Microbiology.

[9] Kushner, S. R. (1996) mRNA decay. In: *Escherichia coli* and *Salmonella thyphymurium*: Cellular and molecular biology (Neidhart, F. C. *et al.* editors) Vol. 1, pp 902-908. Washington D. C., American Society for Microbiology.

[10] McAdams, H. H. & Arkin, A. (1997). Stochastic mechanisms in gene expression. Proc. Natl. Acad. Sci. USA **94,** 814-819.

[11] Caligiuri, M. G. & Bauerle, R. (1990). Identification of amino acid residues involved in feedback regulation of the anthranilate synthase complex from *Salmonella typhimurium*. Biochemistry **34:**13183-13189.

[12] Ardvidson, D. N.; Bruce, C.; & Gunsalus, R. P. (1986). Interaction of the Escherichia coli trp aporepressor with its ligand, L-tryptophan. J. Biol. Chem. **261:**238-243.

[13] Lane, A. N. (1986). The interaction of the trp repressor from Escherichia coli with L-tryptophan and indole propanoic acid. Eur. J. Biochem. **157:**405-413.

[14] Marmostein, R. Q.; Joachimiak, A.; Sprinzl, M.; & Sigler, P. B. (1987). The structural basis for the interaction between L-tryptophan and the Escherichia coli trp aporepressor. J. Biol. Chem. **262:**4922-4927.

[15] Jin, L.; Yang, J.; & Carey, J. (1993). Thermodynamics of ligand binding to trp repressor. Biochemistry **32:**7302-7309

[16] Yanofsky, C.; Horn, V.; & Gollnick, P. (1991) Physiological studies of tryptophan transport and tryptophanase operon induction in *Escherichia coli*. J. Bacteriol. **173:** 6009-6017.

[17] Yanofsky, C. & Horn, V. (1994) Role of regulatory features of the *trp* operons of *E. coli* in mediating a response to a nutritional shift. J. Bacteriol. **176:** 6245-6254.

[18] Vogel, H. J. & Bonner, D. M. (1956). Acetylornithinase of *Escherichia coli*: partial purification and some properties. J. Biol. Chem. **218:** 97-106.

A Repression dynamics

As mentioned in the main body of the present work, free operons (O_F) can be bound by either *mRNA* polymerase molecules (P) or active repressor molecules (R_A). After binding, the *mRNAP-DNA* complex has to undergo a series of isomerizations before it can assemble the first *mRNA* nucleotide. This whole process is assumed to take place with a rate $k_p P M_F(t)$. On the other hand, the repression process is taken as a reversible first order reaction, with forward and backward constant rates k_r and k_{-r}, respectively. All the parameters involved in these processes are estimated in Appendix B and shown in Table 3. They reveal that repression is about two orders of magnitude faster than the binding of *mRNAP*'s to free operons. This fact justifies a quasi-steady state assumption for repression, which implies the following chemical equilibrium equation,

$$k_r O_F(t) R_A(t) = k_{-r} O_R(t), \tag{A.1}$$

where $O_R(t)$ represents the concentration of repressed operons. Let O denote the total operon concentration and O_P the concentration of operons with a *mRNAP* in the controlling section. Assume that *DNA* replication produces enough new *trp* operons to balance dilution so that O keeps constant. Thus, $O = O_F(t) + O_R(t) + O_P(t)$. By solving for $O_F(t)$ from this and Equation A.1 we get:

$$\begin{aligned} O_F(t) &= O - O_P(t) - O_R(t) \\ &= \frac{K_r}{K_r + R_A(t)} \big(O - O_P(t)\big), \end{aligned} \tag{A.2}$$

with $K_r = k_{-r}/k_r$.

After a *mRNAP* binds a free operon and assembles the first *mRNA* nucleotide, it moves along the operon continuing with transcription. It takes a time τ_p (estimated in Appendix B) for a polymerase to move far enough to free the operon controlling section. From this, the binding rate of *mRNAP* to free operons is $k_p P O_F(t)$, while the rate of operons freed by polymerases who have moved far enough equals the rate of *mRNAP*'s that bound free operons a time τ_p ago, times a dilution factor due to the assumption that the bacterial culture is exponentially growing at a rate μ, *i.e.:* $k_p P O_F(t-\tau_p) e^{-\mu\tau_p}$. The equation governing the dynamics of O_P resulting from all this considerations is

$$\frac{dO_P}{dt} = k_p P \big[O_F(t) - OF(t-\tau_p) e^{-\mu\tau_p}\big] - \mu O_P(t). \tag{A.3}$$

The equation for the O_F dynamics can be derived from Equations (A.2) and (A.3) as

$$\begin{aligned} \frac{dO_F}{dt} &= \frac{K_r}{K_r + R_A(t)} \Big\{ \mu O - k_p P \big[O_F(t) - \\ &\qquad O_F(t-\tau_p) e^{-\mu\tau_p}\big] \Big\} - \mu O_F(t). \end{aligned} \tag{A.4}$$

The term $K_r/\big[K_r + R_A(t)\big]$ in the above equation stands for the fraction of non-repressed operons, while the term μO is the operon production rate, which is such that balances dilution in order to keep O constant.

B Parameter estimation

Bremer & Dennis [B.1] reported growth rates of *E. coli* cultures under different temperature and nutrient conditions. These rates vary from $0.6\,\mathrm{h}^{-1}$ to $2.5\,\mathrm{h}^{-1}$. Bliss [B.2] reports experimental results about the kinetics of tryptophan production in *E. coli* cultures. In those experiments, the growth rate is $2.0 \times 10^{-4}\,\mathrm{s}^{-1}$. Here, we employ the smallest growth rate reported by Bremer & Dennis [B.1],

$$\mu \simeq 0.6\,h^{-1} = 1.0 \times 10^{-2}\,\mathrm{min}^{-1},$$

because it is the most likely to correspond to bacteria growing in minimal media (the experiments with which we compare the model in Section 3).

Bremer & Dennis [B.1] further reported average steady-state concentrations of free *mRNA* polymerase molecules (P) and free ribosomes (ρ) at different growth rates. From these data, $P \simeq 1250\,\mathrm{molecules/cell}$ and $\rho \simeq 1400\,\mathrm{molecules/cell}$ for the growth rate considered here. *E. coli* are rod-like bacteria $3-5\,\mu$m long and $0.5\,\mu$m in diameter, so they have volume in the range from 6.0×10^{-16} liters to 9.8×10^{-16} liters. Taking a mean volume of 8.0×10^{-16} liters, the average molar concentrations of free *mRNA* polymerase molecules and ribosomes are calculated to be:

$$P \simeq 2.6\,\mu\mathrm{M},$$

and

$$\rho \simeq 2.9\,\mu\mathrm{M}.$$

From Gunsalus *et al.* [B.3], the normal concentration of aporepressor (R_I) in a tryptophan free culture medium is:

$$\overline{R_I} \simeq 375\,\mathrm{molecules/cell} \simeq 0.75\,\mu\mathrm{M}.$$

In normal *E. coli*, there is only one tryptophan operon O per genome. *E. coli* cells can be genetically manipulated by introducing plasmids of tryptophan

operon so the number of them can be increased up to a few hundred. In the present work, we consider normal cells. When a given cell is undergoing DNA replication, it generally has a complete and a second partially assembled genome. In very rapid growing cultures, it is possible to find two partially assembled genomes in cells undergoing DNA replication. This explains why the average genome equivalents per cell is larger than one. According to Bremer & Dennis [B.1] it is around 1.6. Therefore

$$O \simeq 3.32 \times 10^{-3} \mu\text{M}.$$

Schmitt *et al.* [B.4] studied the activation of the *trp* repressor by tryptophan. In this process, two molecules of tryptophan bind the *trp* repressor in two independent sites with identical affinities and no cooperativity [12, 13, 14, 15]. The corresponding forward and backward reaction rate constants were respectively estimated by Schmitt *et al.* at physiological temperature as:

$$k_t \simeq 3.48 \times 10^2 \, \mu\text{M}^{-1}\text{min}^{-1},$$

and

$$k_{-t} \simeq 2.1 \times 10^4 \, \text{min}^{-1}.$$

The dissociation constant of the tryptophan repressor-operator complex $K_r = k_{-r}/k_r$, was measured by Klig *et al.* [B.5], who report the value $K_r = 2.6 \times 10^{-3} \, \mu\text{M}$. Klig *et al.* also measured the tryptophan repressor-operon complex degradation rate as

$$k_{-r} \simeq 1.2 \times 10^{-2} \, \text{min}^{-1},$$

so k_r is

$$k_r \simeq 4.6 \, \mu\text{M}^{-1}\text{min}^{-1}.$$

Anthranilate synthase is feedback inhibited when two molecules of tryptophan bind each one of the *TrpE* subunits. Caligiuri & Bauerle [11] studied this process and concludes that *Trp* binding is cooperative in the wild type enzyme, with a Hill coefficient of

$$n_H \simeq 1.2.$$

They also estimated the forward (k_i) and backward (k_{-i}) reaction rates as

$$k_i \simeq 1.76 \times 10^{-2} \, \mu\text{M}^{-1}\text{min}^{-1},$$

and

$$k_{-i} \simeq 7.20 \times 10^{-2} \, \text{min}^{-1}.$$

Trp feedback inhibition of *TrpE* activity results in approximately 50% inhibition of *TrpE* activity in cultures growing in the minimal medium, which in turns results in the *trp* operon being expressed twice what it would be if there were no feedback inhibition [B.6]. In our model, the activity of anthranilate synthase is proportional to the non-inhibited enzymatic concentration and its production rate is assumed to be one half that of *TrpE*. Thus, the above mentioned experimental fact may be interpreted as that one half of the anthranilate synthase pool is feedback inhibited by tryptophan in cultures growing in the minimal medium. This is also asserted by Bliss *et al.* [4]. From this and Equation (5) of table 2, which defines the relation between the concentration of active enzymes (E_A) and the total enzymatic pool (E), the *Trp* concentration for bacteria growing in the minimal medium can be calculated as

$$\overline{T} = \frac{k_{-i}}{k_i} \simeq 4.1 \, \mu\text{M}.$$

In this model, we take the normal steady-state conditions to be those of the bacterial culture growing in the minimal medium. Based on this, $\overline{T}$ is the normal steady tryptophan concentration.

From the data reported by Draper [B.7], the translation initiation rate k_ρ is estimated to be in the range from $k_\rho \simeq 60 \, \mu\text{M}^{-1}\text{min}^{-1}$ to $k_\rho \simeq 600 \, \mu\text{M}^{-1}\text{min}^{-1}$. Further, efficient *mRNA*'s have been observed to initiate translation every $3\,\text{s} = 5.0 \times 10^{-2}\,\text{min}$ [B.7]. This implies that

$$\tau_\rho \simeq 5.0 \times 10^{-2} \, \text{min}.$$

Given that initiation is the rate-limiting step of translation [B.7], we must have $k_\rho \overline{\rho} \simeq \tau_\rho^{-1}$. From this, we estimate the value of k_ρ to be

$$k_\rho = \frac{1}{\tau_\rho \rho} \simeq 6.9 \, \mu\text{M}^{-1}\text{min}^{-1}.$$

Mulligan *et al.* [B.8] measured transcription initiation rates for several operons. The values they report range from $0.43 \, \mu\text{M}^{-1}$ to $3,420.0 \, \mu\text{M}^{-1}$. To estimate a proper value for k_p, we use the fact that tryptophan operon allows transcription initiation every $6\,\text{s} = 0.1\,\text{min}$ [B.9]. From this, the time delay τ_p is

$$\tau_p \simeq 0.1 \, \text{min}.$$

Initiation is also the rate limiting process for transcription. i.e. $k_p P = \tau_p^{-1}$. Thus, k_p can be alternately estimated as

$$k_p = \frac{1}{\tau_p P} \simeq 3.9 \mu\text{M}^{-1}\text{min}^{-1}.$$

The *TrpE* polypeptide is 520 amino acids long. This means that the length of the *trpE* gene is 1560

nucleotides long. On the other hand, Bremer & Dennis [B.1] report a *mRNA* chain elongation rate of about 39 Nucleotides/second at the growth rate considered here. From this, τ_e can be estimated as

$$\tau_e \simeq 0.66\,\text{min}.$$

Functional half-lives for different kinds of *mRNA* have been reported [9]. They range from 40 s to 20 min. These imply degradation rates in the range from $3.5 \times 10^{-2}\,\text{min}^{-1}$ to $1.03\,\text{min}^{-1}$. Bliss *et al.* [4] consider a degradation rate of $0.96\,\text{min}^{-1}$. Here, we estimate the *mRNA* degradation rate by making use of the experimental fact that under normal conditions, around 30 ribosomes are bound to a single *mRNA* [B.9]. The binding rate for ribosomes should then be about 30-fold bigger than that for *D*-enzymes. The ribosome binding rate can be estimated as ρk_ρ. Therefore

$$k_d D \simeq \frac{\rho k_\rho}{30} \simeq 0.6\,\text{min}^{-1}.$$

The assumption of constant repressor concentration can be read as $R = R_I + R_A$. This and Equation (6) of Table 2, which determines the concentration of active repressor molecules, permit the estimation of the total repressor concentration as

$$\begin{aligned} R &= \frac{K_t + \overline{T}}{K_t}\overline{R_I} \\ &\simeq 0.8\,\mu\text{M}, \end{aligned}$$

as well as the active repressor steady-state concentration as

$$\begin{aligned} \overline{R_A} &= \frac{\overline{T}}{\overline{T} + K_t} R \\ &\simeq 5.09 \times 10^{-2}\,\mu\text{M}, \end{aligned}$$

where $K_t = k_{-t}/k_t$.

Landick *et al.* [B.10] note that under excess tryptophan conditions, 85% of the *mRNAP*'s initiating transcription halt due to transcriptional attenuation. There is also evidence that transcriptional attenuation is only released under severe tryptophan starvation. The function

$$A\,(T) = b\Big(1 - e^{-T(t)/c}\Big),$$

with

$$b \simeq 0.85$$

and

$$c \simeq 4.0 \times 10^{-2}\,\mu\text{M},$$

satisfies those experimental observations.

Following Bliss *et al.* [4] and Sinha [5], we take the enzyme degradation rate γ to be approximately zero, since according to their estimations, it is much smaller than other terms like the growth rate:

$$\gamma \simeq 0\,\text{min}^{-1}.$$

From the equations that govern the evolution of O_F (Equation (1) of Table 2) the steady-state concentration of free operon controlling sections is

$$\begin{aligned} \overline{O}_F &= \frac{\mu}{k_p P\big(1 - e^{-\mu\tau_p}\big) + \mu\dfrac{K_r + R_A(\overline{T})}{K_r}} O \\ &\simeq 1.54 \times 10^{-4}\,\mu\text{M}. \end{aligned}$$

The normal concentration of free *TrpE*-related ribosome binding sites can be estimated from the steady state solution of the equation for dM_F/dt (Equation (3) of Table 2) as

$$\begin{aligned} \overline{M}_F &= \frac{k_p P e^{-\mu\tau_m}\big[1 - A(T)\big]}{k_\rho \rho\big(1 - e^{-\mu\tau_\rho}\big) + k_d D + \mu}\overline{O}_F \\ &\simeq 3.78 \times 10^{-4}\,\mu\text{M}. \end{aligned}$$

The steady-state concentration of anthranilate synthase enzyme can be calculated from the equation for $dE/dt = 0$ (see Equation (4) of Table 2):

$$\overline{E} = \frac{k_\rho \rho e^{-\mu\tau_e}}{2(\gamma + \mu)}\overline{M}_F \simeq 0.378\mu\text{M}.$$

According to Bliss *et al.* [4], the internal consumption rate of tryptophan can be modeled using a Michaelis-Menten type relation:

$$g\frac{T}{T + K_g}.$$

They also assert that K_g is about or less than one tenth of the normal *Trp* concentration. Following this we have

$$K_g \simeq 0.2\mu\text{M}.$$

The constant g stands for the maximum tryptophan consumption rate. The rate of tryptophan consumption under normal conditions can be estimated by noting that tryptophan is primarily consumed in the assembly of proteins. Bremer and Dennis [B.1] report that the average cell dry weight at the growth rate considered in this work is $148 \times 10^{-9}\,\mu\text{g}$. By multiplying by the growth rate ($\omega \simeq 1 \times 10^{-2}\,\text{min}^{-1}$) and dividing by the average cell volume (8×10^{-16} liters) we get the protein production rate estimated as $1.85\,\text{g liter}^{-1}\text{min}^{-1}$. Since 20 to 25% of the cell dry weight corresponds to protein mass, and noting that tryptophan accounts for around 1% of this dry weight

[4], the tryptophan consumption rate under normal conditions is

$$g\frac{\overline{T}}{\overline{T}+K_g} \simeq 4.63\times10^{-3}\,\mathrm{g\,liter^{-1}min^{-1}} \simeq 22.7\,\mu\mathrm{M\,min^{-1}}.$$

This permits us to estimate g by solving for it in terms of $\overline{T}$, and K_G:

$$g \simeq 25.0\,\mathrm{min^{-1}}.$$

E. coli are capable of efficiently transporting tryptophan from its environment. To achieve this, *E. coli* synthesize three tryptophan permeases. Two of them are specific, whereas the other also transports phenylananine and tyrosine [16]. The expression of the operons that encode these enzymes is dependent, in general, on the tryptophan and tryptophan repressor concentrations. Furthermore the tryptophan permeases may also play the role of maintaining a high intracellular tryptophan concentration when there is no source of extracellular tryptophan. According to Drozdov-Tikhomirov & Skurida [B.11], the tryptophan uptake rate can be modeled by the following equation in terms of the internal and external (T_{ext}) tryptophan concentrations.

$$F(T,T_{\mathrm{ext}}) = d\frac{T_{\mathrm{ext}}}{e+T_{\mathrm{ext}}\left[1+T(t)/f\right]}$$

The value of parameters e and f was also estimated by Drozdov-Tikhomirov & Skurida as

$$e \simeq 0.9\,\mu\mathrm{M},$$

and

$$f \simeq 380\,\mu\mathrm{M}.$$

Parameter d can be estimated from the experimental fact that for bacteria growing in a media with a high tryptophan concentration (where the *Trp* uptake rate is approximately d), the enzyme activity is about one tenth of the activity corresponding to the minimal medium [17]. The value of d compatible with this experimental result is:

$$d \simeq 23.5\,\mu\mathrm{M\,min^{-1}}.$$

The tryptophan production rate constant K can be estimated from the steady state equation for $dT/dt = 0$ (see Equation (9) of Table 2 and notice that $F(T,0) = 0$) as

$$K = \frac{G(\overline{T})+\mu\overline{T}}{E_A(\overline{E},\overline{T})} \simeq 126.4\,\mu M^{-1}\mathrm{min^{-1}}.$$

References

[B.1] Bremer, H. & Dennis, P. P. (1996) Modulation of chemical composition and other parameters of the cell by growth rate. In: *Escherichia coli* and *Salmonella thyphymurium*: Cellular and molecular biology (Neidhart, F. C. et al. editors) Vol. 2, pp 1553-1569. Washington D. C., American Society for Microbiology.

[B.2] Bliss, R. D. (1979) A specific method for determination of free tryptophan and endogenous tryptophan in *Escherichia coli*. Analyt. Biochem. **93:** 390-398.

[B.3] Gunsalus, R. P.; Miguel, A. J.; & Gunsalus, G. L. (1986). Intracellular *Trp* repressor levels in *Escherichia coli*. J. Bacteriol. **167:**272-278.

[B.4] Schmitt, T. H.; Zheng, Z; & Jardetzky, O. (1995). Dynamics of tryptophan binding to *Escherichia coli Trp* repressor wild type and AV77 mutant: An NMR study. Biochemistry **34:**13183-13189.

[B.5] Klig, L. S.; Crawford, I. P.; and Yanofsky, C. (1987) Analysis of *trp* repressor-operator interaction by filter binding. Nucl. Acids Res. **15:** 5339-5351.

[B.6] Yanofsky, C. (2000). Personal communication.

[B.7] Draper, D. E. (1996) Translational initiation. In: *Escherichia coli* and *Salmonella thyphymurium*: Cellular and molecular biology (Neidhart, F. C. et al. editors) Vol. 1, pp 849-860. Washington D. C., American Society for Microbiology.

[B.8] Mulligan, M. E.; Hawley, D. K.; Entriken, R.; & McClure, W. R. (1984) *Escherichia coli* promotes sequences predict in vitro RNA polymerase activity. Nucl. Acids Res. **12:** 789-800.

[B.9] Yanofsky, C. & Crawford, I. P. (1987). The tryptophan operon. In: *Escherichia coli* and *Salmonella thyphymurium*: Cellular and molecular biology (Neidhart, F. C. et al. editors) Vol. 2, pp 1454-1472. Washington D. C., American Society for Microbiology.

[B.10] Landick, R.; Turnbough, C. L.; & Yanofsky, C. (1996) Transcription attenuation. In: *Escherichia coli* and *Salmonella thyphymurium*: Cellular and molecular biology (Neidhart, F. C. et al. editors) Vol. 1, pp 1263-1286.

[B.11] Drozdov-Tikhomirov, L. N. & Skurida, G. I. (1977). Mathematical model of tryptophan synthesis and excretion into the environment by *E. coli* cells. Mol. Biol. (Mosk) **11:**843-853.